



ELSEVIER

Available online at www.sciencedirect.com

SCIENCE @ DIRECT®

Journal of Magnetism and Magnetic Materials 300 (2006) e294–e297

www.elsevier.com/locate/jmmm

SQUID-measurements of relaxation time of Fe₃O₄ superparamagnetic nanoparticle ensembles

I. Volkov^{a,*}, S. Gudoshnikov^{b,c}, N. Usov^{b,c}, A. Volkov^d, M. Moskvina^d, A. Maresov^a,
O. Snigirev^a, S. Tanaka^e

^aPhysics Department of Moscow State University, Moscow 119992, Russia

^bInstitute of Terrestrial Magnetism, Ionosphere and Radio Wave Propagation RAS (IZMIRAN), Troitsk, Moscow region 142190, Russia

^cMagnetic and Cryoelectronic Systems Ltd., 4/1, Bozhenko Street, Moscow 121351, Russia

^dChemical Department of Moscow State University, Moscow 119992, Russia

^eToyohashi University of Technology, Toyohashi, Japan

Available online 15 November 2005

Abstract

High- T_C scanning SQUID magnetometer is applied for measuring the magnetization relaxation of the ensembles of spherical colloidal Fe₃O₄ nanoparticles dispersed in the rigid polymer matrix preventing nanoparticles from agglomeration. According to the transmission electron microscopy data, the size distribution of nanoparticles is well described by the Gaussian profile with the mean size and the dispersion of about 7.5 and 2.3 nm, respectively. High sensitivity of SQUID magnetometer allows us to study samples at low contents of the magnetic component (0.1–1.0 vol%) magnetized in low magnetic field ($\sim 10^{-4}$ T) produced by a low-inductance coil with short switching time (12 μ s). A low content of the magnetic component provides the absence of interparticle dipolar interactions, thus simplifying significantly the theoretical description of the magnetization relaxation process. The measured magnetization relaxation curves are found to be in reasonable agreement with the numerical simulation data.

© 2005 Elsevier B.V. All rights reserved.

PACS: 75.20.-g; 85.25.Dq; 75.50.Tt; 75.40.Mg

Keywords: Magnetic nanoparticles; Superparamagnetic relaxation; SQUID magnetometry; Numerical simulation

The magnetic nanomaterials come into ever increasing use in various areas of science and technology. Magnetic storage of information [1,2] and immunoassays utilizing magnetic labeling technique [3,4] are one of the most advanced applications of magnetic nanomaterials. In order to predict and analyze the behavior of single-domain nanoparticles, one must take into account the superparamagnetic phenomena occurred due to thermally activated switching of their magnetic moments. In this context, SQUID magnetometry has been successfully applied to measure the switching times of individual nanoparticles [5,6] and the spontaneous magnetic noise arising in films of self-assembled Co nanoparticles [7].

In the present paper, the high- T_C scanning SQUID magnetometer [8] is used to measure the magnetization relaxation curves of a dilute ensemble of spherical Fe₃O₄ nanoparticles. A series of samples with the mean size of nanoparticles of about 7 nm was studied. The nanoparticles were dispersed in the rigid polymer matrix (polyvinyl alcohol + chitosan) preventing them from agglomeration. The low content of the magnetic component (0.2 vol%) in the samples enabled us to neglect the interparticle dipolar interactions in the theoretical analysis. The transmission electron microscopy (TEM) was used to determine the size distribution of magnetic nanoparticles and to control the homogeneity of their spatial distribution in the matrix. According to the TEM image presented in Fig. 1, the ensemble consists of well-separated particles with near-spherical shape. Note that the areas of irregular shape in this image are caused by the overlap of projections of

*Corresponding author. Tel.: +7 095 939 3343; fax: +7 095 939 3000.

E-mail address: volkov256@yandex.ru (I. Volkov).

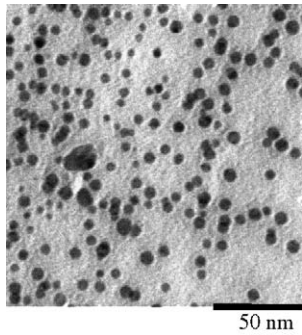


Fig. 1. TEM image of Fe_3O_4 nanoparticles dispersed in the rigid polymer matrix at a content of 0.5 vol%.

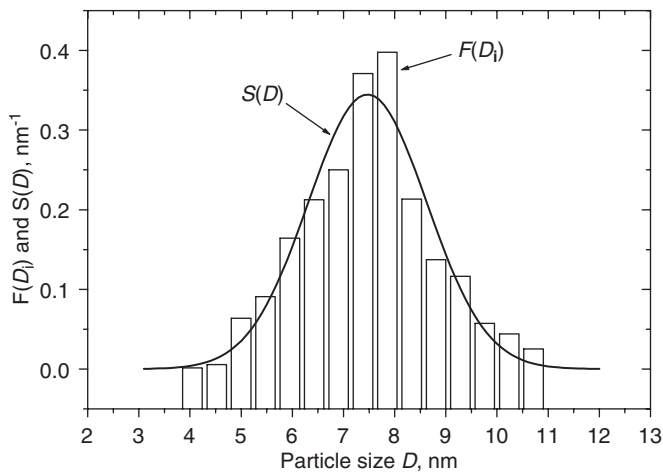


Fig. 2. Discrete $F(D_i)$ and continuous $S(D)$ functions of the size distribution of the volume fraction of magnetic component.

particles located at different heights. Fig. 2 shows the size distribution histogram $F(D_i)$ approximated by a normalized Gaussian profile $S(D)$ with the mean diameter $D_0 = 7.47$ nm and the dispersion $\sigma = 2.32$ nm.

The SQUID sensors were fabricated from high- T_c superconductor films ($\text{YBa}_2\text{Cu}_3\text{O}_x$) deposited on SrTiO_3 bicrystal substrates with misorientation angles of 24° and 30° . The fabrication process included photo- and e-beam lithographies followed by wet and ion beam etchings [9–11]. The SQUIDs had a geometry of square washer with the following parameters: the hole dimension $40\ \mu\text{m}$ and the outer dimension $120\ \mu\text{m}$.

The magnetization relaxation measurements were performed on the samples with dimensions of $0.6 \times 0.6 \times 0.06\ \text{mm}^3$. The SQUID sensor was located close to the sample surface at a height of about $300\ \mu\text{m}$. The SQUID plane was roughly parallel both to the sample surface and to the applied field direction. The measurements were carried out at a temperature of $T = 77\ \text{K}$ inside a μ -metal shield with the remanent magnetic field as high as $10^{-7}\ \text{T}$. In order to magnetize the sample, a weak external magnetic field ($\sim 68\ \text{A/m}$) generated by a coil was applied parallel to the sample surface. After several minutes allowing the

sample magnetization to attain its equilibrium, the SQUID sensor scanned the z -component of the stray magnetic field $B_z(x, y)$ produced by the sample and the obtained data were saved in the file. Finally, the SQUID sensor was located at the maximum of B_z -component (close to the sample edge) and the external magnetic field was switched off. Note that the initial sample magnetization was quantitatively retrieved from the $B_z(x, y)$ data using mathematical procedure mentioned in Ref. [12].

In order to switch off the magnetizing field, a special electronic circuit was designed. It enabled us to switch off the bias current flowing through the coil to within 300 ns. Since the residual current and residual magnetic field cannot become zero immediately after the bias current is switched off, the following condition must be fulfilled: the magnetizing field must relax much faster than the sample magnetization. In our experiment, we have achieved a relaxation time of the external field (99% decay of the magnitude) of about $12\ \mu\text{s}$. After a $12\text{-}\mu\text{s}$ time gap, we started registration of useful relaxing signal produced by the sample. Within this time gap, the amplitude of the useful signal decreased from 5% to 20% of its initial value. Nevertheless, the measured portion of the relaxation curves contained very useful information on the distribution of the relaxation times in the ensemble under investigation. Curve 1 in Fig. 3 demonstrates the measured magnetization relaxation of the Fe_3O_4 ensemble (0.2 vol%) presented in the logarithmic time scale.

In order to understand the experimental results obtained, we have calculated the relaxation curves of Fe_3O_4 nanoparticles with diameters D in the range from 5 to 11 nm corresponding to the size distribution histogram presented in Fig. 2. At $T = 77\ \text{K}$, below the Verwey's transition temperature $T_v = 125\ \text{K}$, the particles are supposed to be roughly uniaxial with the magnetocrystalline anisotropy constant $K_u = 4.5 \times 10^4\ \text{J/m}^3$ and the

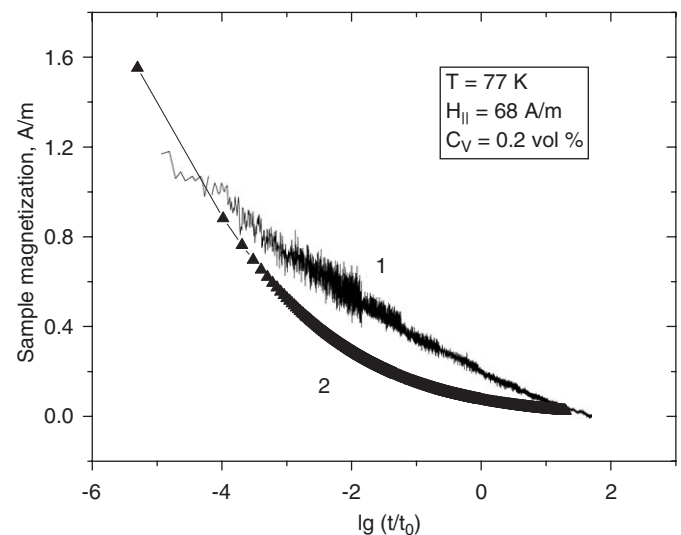


Fig. 3. Magnetization relaxation in the dilute ensemble of Fe_3O_4 nanoparticles presented in logarithmic time scale: (1) experimental data; (2) numerical simulation result.

Table 1
Reduced energy barriers, relaxation times and average magnetization of Fe₃O₄ nanoparticles at $T = 77$ K

D , nm	5	6	7	8	9	10	11
$K_u V/k_B T$	2.77	4.79	7.61	11.35	16.16	22.17	29.51
τ , s	5.4×10^{-9}	3.1×10^{-8}	4.1×10^{-7}	1.4×10^{-5}	1.5×10^{-3}	0.51	680
$\langle M \rangle / M_s$	1.9×10^{-3}	4.0×10^{-3}	7.2×10^{-3}	1.1×10^{-2}	1.7×10^{-2}	2.4×10^{-2}	3.2×10^{-2}

saturation magnetization $M_s = 5 \times 10^5$ A/m [13]. For smaller diameters, $5 < D < 8$ nm, the calculations were made by means of direct integration of the Landau—Lifshitz equation augmented by a stochastic thermal field with a white noise spectrum [14–16]. For larger particles, $9 < D < 11$ nm, the analytical estimate [17] for the relaxation time has been used, because for these sizes the numerical simulation is time consuming. Table 1 summarizes the reduced energy barriers $\varepsilon = K_u V/k_B T$ (V is the particle volume and k_B is the Boltzmann constant), relaxation times and equilibrium particle magnetizations in applied magnetic field with the magnitude of 68 A/m as a function of particle size D . Note that for the given ensemble, the highest relaxation time corresponds to particles with $D = 11$ nm, because the percentage of particles with $D > 11$ nm is negligibly small. The highest relaxation time turns out to be of the order of exposition time of the ensemble in applied magnetic field ($t_{\text{exp}} \sim 300$ s). Therefore, practically all particles of the ensemble attain their equilibrium magnetizations during the exposition time. The forth row of the Table 1 gives, in fact, the magnetization susceptibility of the particles as a function of their diameters at $T = 77$ K.

Fig. 3 shows the measured magnetization relaxation curve 1 for the dilute ensemble of Fe₃O₄ nanoparticles in comparison with the numerical simulation result (curve 2) presented in the logarithmic time scale with $t_0 = 1$ s. The time interval of the measurement is given by 50 s and the initial time gap is 12 μ s in this case. The volume fraction of the magnetic component of the ensemble is $C_V = 0.2$ vol%. Similar data were also obtained for the ensembles with $C_V = 0.5$ and 1.0 vol%, though the characteristic relaxation time increased with increasing content of magnetic component due to interparticle dipolar interactions.

The theoretical relaxation curves of the ensembles under study were obtained by convoluting the calculated relaxation curves for the particles with given $D = 5$ –11 nm with the size distribution histogram presented in Fig. 2. According to Fig. 1, the shapes of the particles are near spherical. Thus, in a good approximation one can neglect the shape anisotropy of the particles. Besides, the mean distance between the particles is estimated to be $\sim 6 D_0$ for $C_V = 0.2$ vol%, where $D_0 \approx 7$ nm is the mean particle diameter. Therefore, the energy of interparticle dipolar interaction is minor as compared to the anisotropy energy. The calculations have been carried out for small values of the damping parameter, $\kappa = 0.01$ –0.05, because there is an

indication [18] that the low-damping regime better corresponds to the experimental situation for an ensemble of perfect magnetic nanoparticles. It is found that the dependence of the relaxation curve 2 on this parameter is minor within this interval. On the other hand, the theoretical relaxation curve depends considerably on the value of uniaxial magnetocrystalline anisotropy constant. One can see from the Fig. 3 that for assumed value of $K_u = 4.5 \times 10^4$ J/m³ [13] there is a reasonable agreement between the experimental and numerical simulation data.

In conclusion, high-sensitive scanning high- T_C SQUID-magnetometer is used to measure the magnetization relaxation curves of a dilute ensemble of Fe₃O₄ nanoparticles at $T = 77$ K. This technique enables us to study samples at low contents of magnetic component (0.1–1.0 vol%) magnetized in a weak magnetic field of the order of 10^{-4} T. The TEM is applied to determine the size distribution of magnetic nanoparticles and to control the homogeneity of their spatial distribution in the matrix. The size distribution of nanoparticles is described well by Gaussian profile with the mean size and the dispersion of about 7.5 and 2.3 nm, respectively. The measured relaxation curves of the dilute ensembles are shown to be in reasonable agreement with the numerical simulation results obtained by means of direct integration of the Landau—Lifshitz equation augmented by a stochastic thermal field with a white noise spectrum.

This work was supported by the ISTC project # 1991.

References

- [1] D. Weller, A. Moser, IEEE Trans. Magn. 35 (1999) 4423.
- [2] www.research.ibm.com/resources/news/20001207_mramimages.shtml
- [3] R. Kötitz, W. Weitschies, L. Trahms, W. Brewer, W. Semmler, J. Magn. Magn. Mater. 194 (1999) 62.
- [4] S. Katsura, T. Yasuda, K. Hirano, A. Mizuno, S. Tanaka, Supercond. Sci. Technol. 14 (2001) 1131.
- [5] W. Wernsdorfer, E.B. Orozco, K. Hasselbach, A. Benoit, B. Barbara, N. Demoncey, A. Loiseau, H. Pascard, D. Mailly, Phys. Rev. Lett. 78 (1997) 1791.
- [6] M. Jamet, W. Wernsdorfer, C. Thirion, D. Mailly, V. Dupuis, P. Mélinon, P. Pérez, Phys. Rev. Lett. 86 (2001) 4676.
- [7] S.I. Woods, J.R. Kirtley, Sh. Sun, R.H. Koch, Phys. Rev. Lett. 87 (2001) 137205.
- [8] S. Gudoshnikov, L. Matveets (Eds.), High-Temperature Superconductivity 2, Springer, Germany, 2004. p. 337.
- [9] I. Volkov, A. Kalabukhov, O. Snigirev, A. Zherikhin, IEEE Trans. Appl. Supercond. 11 (2001) 292.

- [10] I. Volkov, A. Kalabukhov, O. Snigirev, A. Zherikhin, *Physica C* 372–376 (2002) 72.
- [11] I. Volkov, M. Chukharkin, O. Snigirev, *IEEE Trans. Appl. Supercond.* 13 (2003) 861.
- [12] I. Volkov, M. Chukharkin, O. Snigirev, A. Volkov, M. Moskvina, S. Gudoshnikov, A. Kerimov, *IEEE Trans. Appl. Supercond.*, 2005, in press.
- [13] S. Chikazumi, *Physics of Magnetism*, Wiley, New York, 1964.
- [14] J.L. Garcia-Palacios, F.J. Lazaro, *Phys. Rev. B* 58 (1998) 4937.
- [15] W. Scholz, T. Schrefl, J. Fidler, *J. Magn. Magn. Mater.* 233 (2001) 296.
- [16] D.V. Berkov, *IEEE Trans. Magn.* 38 (2002) 2489.
- [17] W.F. Brown Jr., *Phys. Rev.* 130 (1963) 1677.
- [18] J.L. Dormann, F. D’Orazio, F. Lucari, E. Tronc, P. Prene, J.P. Jolivet, D. Fiorani, R. Cherkaoui, M. Nogues, *Phys. Rev. B* 53 (1996) 14291.